

Barycentric rational approximation for learning the index of a dynamical system from limited data

Davide Pradovera* Ion Victor Gosea[†] Jan Heiland[‡]

*Department of Mathematics, KTH Royal Institute of Technology, Lindstedtsvägen 25, 11428, Stockholm, Sweden.

Email: davidepr@kth.se, ORCID: [0000-0003-0398-1580](https://orcid.org/0000-0003-0398-1580)

[†]Max Planck Institute for Dynamics of Complex Technical Systems, Sandtorstr. 1, 39106 Magdeburg, Germany.

Email: gosea@mpi-magdeburg.mpg.de, ORCID: [0000-0003-3580-4116](https://orcid.org/0000-0003-3580-4116)

[‡]Ilmenau University of Technology, Weimarer Str. 25, 98693 Ilmenau, Germany and Max Planck Institute for Dynamics of Complex Technical Systems, Sandtorstr. 1, 39106 Magdeburg, Germany

Email: jan.heiland@tu-ilmenau.de, ORCID: [0000-0003-0228-8522](https://orcid.org/0000-0003-0228-8522)

Abstract: We consider the task of data-driven identification of dynamical systems, specifically for systems whose behavior at large frequencies is non-standard, as encoded by a non-trivial *relative degree* of the transfer function or, alternatively, a non-trivial *index* of a corresponding realization as a descriptor system. We develop novel surrogate modeling strategies that allow state-of-the-art rational approximation algorithms (e.g., AAA and vector fitting) to better handle data coming from such systems with non-trivial relative degree. Our contribution is twofold. On one hand, we describe a strategy to build rational surrogate models with *prescribed relative degree*, with the objective of mirroring the high-frequency behavior of the high-fidelity problem, when known. The surrogate model's desired degree is achieved through constraints on its barycentric coefficients, rather than through ad-hoc modifications of the rational form. On the other hand, we present a degree-identification routine that allows one to estimate the *unknown relative degree* of a system from low-frequency data. By identifying the degree of the system that generated the data, we can build a surrogate model that, in addition to matching the data well (at low frequencies), has enhanced extrapolation capabilities (at high frequencies). We showcase the effectiveness and robustness of the newly proposed method through a suite of numerical tests.

Keywords: rational approximation, system identification, data-driven approach, AAA algorithm, barycentric form, descriptor systems, frequency domain, transfer function

Novelty statement: In this work, state-of-the-art rational-approximation algorithms are tailored to the approximation of classes of dynamical systems, whose behavior at large frequencies is not proper, e.g., systems modeled as descriptor systems through differential-algebraic equations. We develop strategies to enable the construction of surrogate models with given relative degree, without destroying the standard barycentric form. We also describe how to automatically detect the relative degree of a system from low-frequency measurements of its frequency response.

1. Introduction

The approximation of large-scale dynamical systems [3] is dire for achieving various goals such as employing efficient simulation or devising robust, automatic control laws. Mode order reduction

(MOR) is a collection of techniques for reducing the computational complexity of mathematical models in numerical simulations. With the ever-developing technology in many engineering fields, more and more complex mathematical models need to be numerically simulated to get deeper insights into the physics of many applied problems. In this framework, MOR aims to construct cheap and fast, but also reliable and accurate surrogate models for the original complex mathematical problem (described by convoluted, coupled, or highly nonlinear dynamical laws). Historically, MOR methods were typically intrusive, as explicit access to the latter models was typically required to compute the reduced-order counterparts. However, in the last decade, increased effort was allocated to the computation of surrogate models in a non-intrusive fashion, i.e., by using data-driven approaches, rather than projection-based ones.

Data-driven (non-intrusive) techniques represent a viable alternative to classical (intrusive) methods of MOR, which rely on explicit access to the large-scale model. Unlike intrusive methods, data-driven surrogate models do not require explicit knowledge of the problem structure or matrices. Instead, low-order models can be directly computed from data, such as snapshots of the system’s state-space evolution, alongside the control inputs and, optionally, the observed outputs.

Frequency domain analysis methods are used to approximate and analyze the behavior of a dynamical system using its transfer function, a system-invariant quantity that does not depend on the system’s states or variables, but only on the input-output map that encodes the “true dimensionality” of the problem. For finite-dimensional linear time-invariant systems, the transfer function is a rational function, whereas infinite-dimensional systems (e.g., delayed or integro-differential ones) lead to more complex irrational structures. By approximating the transfer function of a large-scale system, one can provide insight on the system’s response to a specific range of frequencies actuated by the control input. The class of methods that are aiming at this can be thought of as rational approximation tools that provide various techniques for an accurate data fit. A standard way of achieving this is by means of *interpolation*, although one must move beyond ill-conditioned classical methods involving polynomials. Instead, through *rational interpolation*, especially when using the *barycentric* form, one can recover both approximation quality and good conditioning [11].

One notable approach for rational interpolation is based on Loewner matrices, was originally presented in [4] and will be referred to as the Antoulas-Anderson (AA) method. A rational interpolant in barycentric form is built by computing the null space of a Loewner matrix based on the available data. Another method is the vector fitting (VF) algorithm [20], which uses a linearized least-squares fitting approach. This algorithm iteratively adjusts some parameters of the rational functions (namely, the support points, as defined below) to minimize the mismatch between the model and the actual data, resulting in an accurate recovery of the transfer function. On the other hand, the adaptive AA (AAA) algorithm [26] combines elements of both approaches, blending interpolation and least-squares fitting. It aims at finding a rational approximant by iteratively adjusting the model based on greedily selected interpolation points and on a least-squares fit.

1.1. The barycentric form

What all the above methods actually have in common is the barycentric form used to express the rational approximation. It is an alternative to other representations of transfer functions, e.g., as the ratio of two polynomials or, as in the “Heaviside” pole-residue format, as the sum of simple fractions. The barycentric form is a numerically stable representation [11] of the rational approximant to be computed. It represents a rational function as the ratio of two sums of fractions with identical singularities (or poles):

$$r(s) = \sum_{k=0}^m \frac{n_k}{s - s_k} \bigg/ \sum_{k=0}^m \frac{d_k}{s - s_k}. \quad (1)$$

The poles of both numerator and denominators, namely, the set $\{s_k\}_{k=0}^m$, are referred to as *support points*. The numerators are different, containing the so-called *barycentric weights* n_k and d_k . One of the most useful features of the barycentric form is that one can encode *interpolation* properties in its structure, in a numerically stable way. Specifically, the value of r at each support point s_k equals n_k/d_k by design. As such, enforcing an arbitrary value f_k at any support point is as easy as setting the numerator barycentric coefficient n_k as $n_k := d_k f_k$. If this is done at all support

points, one obtains the *interpolatory* barycentric form

$$r(s) = \frac{\sum_{k=0}^m \frac{w_k f_k}{s - s_k}}{\sum_{k=0}^m \frac{w_k}{s - s_k}}, \quad (2)$$

which attains $r(s_k) = f_k$ for all k . Note that, for historical reasons, we have switched to the symbol w_k to denote the denominator barycentric weights.

It is well known that r in either barycentric form (1) or (2) is a rational function of *rational type* (m, m) , i.e., r may be expressed as the ratio of two complex-valued polynomials, each of degree at most m . In order to obtain this alternative form, it suffices to multiply both numerator and denominator by the nodal degree- $(m + 1)$ polynomial $\pi(s) = \prod_{k=0}^m (s - s_k)$. This leads to the “rational” (as opposed to “barycentric”) form of r :

$$r(s) = \frac{\sum_{k=0}^m n_k L_k(s)}{\sum_{k=0}^m d_k L_k(s)} \text{ or } r(s) = \frac{\sum_{k=0}^m w_k f_k L_k(s)}{\sum_{k=0}^m w_k L_k(s)}, \quad (3)$$

for (1) and (2), respectively. Above, $L_k(s) = \pi(s)/(s - s_k)$ is a degree- m “non-normalized” Lagrange polynomial. The rational form of r is often avoided due to how unstable the evaluation of the polynomials L_k generally is. On the other hand, the barycentric form is preferred due to its more beneficial numerical properties.

1.2. Motivation: DAE index and relative degree

In this work, we will show how, by imposing extra conditions on the barycentric weights appearing in (1) and (2), one can achieve a prescribed rational type. To be more precise, we will focus on prescribing a certain (*relative*) *degree* for the rational function, defined as the difference between the degrees of numerator and denominator in polynomial form.

This quantity is of interest, e.g., in the study of descriptor systems characterized by differential-algebraic equations (DAEs). Indeed, while a standard ODE system (without a *feedthrough term*) has a transfer function with relative degree at most -1 , the transfer function of a linear DAE can contain terms of higher relative degree, often referred to as *polynomial* or *improper part*, dominating the response at high frequencies. We refer the reader to [28, 24] for more in-depth characterization, properties, and solutions of DAE systems. In the literature of DAEs, a concept closely related to relative degree is that of *index*. Although various different concepts of index exist, we will casually use the term “DAE index” to denote the relative degree plus one. This is correct if one refers to the *Kronecker* index, assuming it to be defined and that there is no realization of smaller index. Concerning the ultimate motivation for our work, we note that the knowledge of the DAE index of a system is fundamental for controller design and MOR [9, 8].

In recent years, there have been attempts to estimate the DAE index from frequency response data. In [19, 5], the coefficients of the polynomial part of the transfer function are estimated from samples at high frequency. Moreover, a method that is tailored for fitting DAEs of index 2 (i.e., relative degree 1) was recently proposed in [18], extending the AA procedure. There, the standard barycentric form was modified, adding an extra weight to the barycentric numerator, as a way to account for the polynomial part of the transfer function.

However, all these methods are characterized by two main shortcomings: (i) the target relative degree must be set in advance, requiring an expert opinion on (an upper bound for) the DAE index, and (ii) they either require modifying the barycentric form or estimating the polynomial coefficients separately. Also, we note that these methods are tailored to positive relative degree, corresponding to the class of DAE systems.

In this contribution, we explicitly address the aforementioned shortcomings, and aim at developing a fully automatic method that uses the standard, unaltered barycentric form to estimate the relative degree of a system’s transfer function given only limited data. Notably, such data is in the form of transfer function samples, which are *not* assumed to be at high-frequency values. For the sake of versatility, we mainly follow the AAA algorithm, which chooses the interpolation points adaptively. In this sense, our contribution may also be viewed as an extension of the AAA algorithm, although our presentation is also relevant for other rational approximation techniques.

Finally, the method proposed here can be applied to both positive and negative relative degrees, regardless of how large or small they are.

The paper is structured as follows: Section 2 reviews rational approximation, including AAA as an exemplifying framework. In Section 3, we rigorously derive algebraic conditions that relate a rational function's relative degree to its barycentric weights. Such theoretical results are first used in Section 4 to devise an algorithm for building a rational approximant of prescribed degree, and then in Section 5 to develop a procedure for data-driven identification of a dynamical system's relative degree. Our novel methods are then numerically tested in Section 7 on a variety of numerical examples, including several MOR benchmarks.

2. Rational approximation using the barycentric form

In this section, we summarize established rational approximation methods that have also been used as model reduction tools throughout the years.

Among the above-mentioned methods, both AA and AAA are interpolatory, i.e., they use form (2), with interpolation being enforced at all support points. As a consequence, the support points must be chosen as a subset of the sample points. The main difference between AA and AAA is that AA fixes the support points in advance, while AAA selects them adaptively through an iterative procedure.

On the other hand, VF is not interpolatory and thus makes use of the general barycentric form (1). The support points are iteratively updated, through the so-called Sanathanan-Koerner (SK) iterations, with the objective of finding their "optimal" location. The number of support points stays constant and must be fixed in advance, as opposed to AAA, where it gradually increases.

In our discussion, we look at all the above methods as approaches for rational approximation (or "surrogate modeling") of a scalar function $f : \mathbb{C} \rightarrow \mathbb{C}$, representing, in our application, the transfer function of a large-scale, complex dynamical system. The to-be-approximated function f is sampled at a set of $m' > 0$ points $\{s'_j\}_{j=1}^{m'}$. These are typically located on the imaginary axis $i\mathbb{R}$ whenever the task involves the identification of dynamical systems from frequency-domain measurements.

Within each iteration of AAA and VF, an optimization problem is used to characterize the barycentric weights of the rational approximant. In its more general formulation, this problem is the same one that must be solved (only once) in AA as well. Specifically, one tries to find the barycentric weights that minimize the ℓ^2 approximation error at the sample points, namely,

$$e := \left(\sum_{j=1}^{m'} \left| f(s'_j) - \frac{\sum_{k=0}^m \frac{n_k}{s'_j - s_k}}{\sum_{k=0}^m \frac{d_k}{s'_j - s_k}} \right|^2 \right)^{1/2}.$$

Due to the nonlinearity of this target function (with respect to d_k), a linearized version of the problem is considered: multiplying by the surrogate denominator leads to

$$\begin{aligned} \min_{n_0, \dots, n_m, d_0, \dots, d_m \in \mathbb{C}} & \sum_{j=1}^{m'} \lambda_j \left| \sum_{k=0}^m \frac{f(s'_j) d_k - n_k}{s'_j - s_k} \right|^2, \\ \text{such that} & \sum_{k=0}^m |d_k|^2 = 1. \end{aligned} \quad (4)$$

Note the addition of a normalization constraint, to avoid the trivial solution $n_k = d_k = 0$ for all k , as well as the presence of the weights λ_j , which are equal to 1 in AA and AAA, while they vary throughout the SK iterations in VF.

In the interpolatory approaches (AA and AAA), the imposition of interpolation conditions reduces the number of degrees of freedom, eliminating the numerator weights, cf. (2). The corre-

sponding optimization problem reads

$$\begin{aligned} \min_{w_0, \dots, w_m \in \mathbb{C}} & \sum_{j=1}^{m'} \left| \sum_{k=0}^m \frac{f(s'_j) - f_k}{s'_j - s_k} w_k \right|^2, \\ \text{such that} & \sum_{k=0}^m |w_k|^2 = 1. \end{aligned} \quad (5)$$

Both (4) and (5) can be solved by standard techniques from computational linear algebra, e.g., through singular value decomposition (SVD), cf. Section 4.

As mentioned above, we will focus on the AAA algorithm in our upcoming presentation, although generalizations to other techniques like VF are possible, as described in Section 6. Our choice is due to AAA's great effectiveness and flexibility. Indeed, the AAA algorithm, originally proposed in [26], has since been extended and developed in recent years, including applications to nonlinear eigenvalue problems [25, 22, 30, 21], MOR of parameterized linear dynamical systems [27, 32], MOR of linear systems with quadratic outputs [16], rational approximation of periodic functions [7], and rational approximation of matrix-valued functions [14, 17, 6, 13].

The characterizing feature of the AAA algorithm is its greedy choice of support points. These are incrementally selected through an iterative procedure, terminating as soon as the ℓ^∞ approximation error, namely, $\max_{j=1, \dots, m'} |r(s'_j) - f(s'_j)|$, is below a user-defined tolerance $\varepsilon_{\text{AAA}} > 0$. A pseudo-code formulation of the AAA algorithm is provided in a later section, namely, Algorithm 1 with $\delta = 0$.

3. Relative degree of barycentric forms

We investigate here how a rational function's degree can be found, based on the function's barycentric coefficients.

We begin by pointing out that the rational type (m, m) of the rational function r in (1) or (2) may not be "exact", i.e., the degrees of the numerator and denominator appearing in the rational form of r may be smaller than m . Following this observation, we rigorously define the relative degree $\text{rdeg}(r)$ of r as the difference between the exact degrees of numerator and denominator of r in the form (3). An equivalent definition involves an asymptotic analysis:

$$r(s) = \mathcal{O}\left(s^{\text{rdeg}(r)}\right) \quad \text{as } s \rightarrow \infty.$$

Remark 3.1. In systems theory, one defines the relative degree of a *system* (as opposed to that of a rational function) by an abuse of notation, as the relative degree of its transfer function (see, e.g., [23, Ch. 4.1]). Generalizations for nonlinear systems are also possible.

We recall that one of our ultimate objectives is building rational functions of given relative degree, in order to well approximate the high-fidelity model's behavior for large frequencies. Accordingly, it is crucial to be able to relate the relative degree $\text{rdeg}(r)$ to the support values f_0, \dots, f_m and to the barycentric weights w_0, \dots, w_m . To this aim, we first derive a useful technical identity.

Lemma 3.1. *Let $\{\alpha_k\}_{k=0}^m \cup \{s_k\}_{k=0}^m \subset \mathbb{C}$. If $|s| > \max_{k=0, \dots, m} |s_k|$, we have the series representation*

$$\sum_{k=0}^m \frac{\alpha_k}{s - s_k} = \sum_{l=0}^{\infty} \left(\sum_{k=0}^m \alpha_k s_k^l \right) \frac{1}{s^{l+1}}. \quad (6)$$

Proof. The claim follows by the Laurent expansion of the geometric series:

$$\frac{1}{s} \sum_{k=0}^m \frac{\alpha_k}{1 - s_k/s} = \frac{1}{s} \sum_{k=0}^m \alpha_k \sum_{l=0}^{\infty} \left(\frac{s_k}{s} \right)^l = \sum_{l=0}^{\infty} \left(\sum_{k=0}^m \alpha_k s_k^l \right) \frac{1}{s^{l+1}}.$$

The requirement that $|s| > |s_k|$ for all $k = 0, \dots, m$ is necessary for the (absolute) convergence of all $(m + 1)$ geometric series. \square

We are now ready to state our main results, starting from the following theorem. We mention that, during the writing of this work, we became aware of a similar 25-year-old result appearing in [10].

Theorem 3.2. *Let μ and ν be non-negative integers $\leq m$ such that*

$$\begin{cases} \sum_{k=0}^m w_k f_k s_k^l = 0 & \text{for } l = 0, 1, \dots, \mu - 1, \\ \sum_{k=0}^m w_k f_k s_k^\mu \neq 0, \end{cases} \quad (7)$$

and

$$\begin{cases} \sum_{k=0}^m w_k s_k^l = 0 & \text{for } l = 0, 1, \dots, \nu - 1, \\ \sum_{k=0}^m w_k s_k^\nu \neq 0. \end{cases} \quad (8)$$

Then the rational function r in (2) has exact type $(m - \mu, m - \nu)$, and its relative degree is $\text{rdeg}(r) = \nu - \mu$.

Except for trivial cases ($w_k f_k = 0$ for all k or $w_k = 0$ for all k), the converse also holds true: if the exact type of r is $(m - \mu, m - \nu)$, then (7) and (8) hold.

Proof. We rely on the representation of r in the rational form (3). For the sake of brevity, we will only prove results for the denominator

$$q(s) = \sum_{k=0}^m w_k L_k(s) = \pi(s) \sum_{k=0}^m \frac{w_k}{s - s_k}.$$

The equivalent results concerning the numerator $p(s) = \sum_{k=0}^m w_k f_k L_k(s)$ follow by the same arguments, by simply replacing any instance of “ w_k ” with “ $w_k f_k$ ”.

Consider

$$d(s) = \frac{q(s)}{\pi(s)} = \sum_{k=0}^m \frac{w_k}{s - s_k}.$$

By Lemma 3.1,

$$d(s) = \sum_{l=0}^{\infty} \left(\sum_{k=0}^m w_k s_k^l \right) \frac{1}{s^{l+1}}$$

as $s \rightarrow \infty$. On the other hand, the nodal polynomial π satisfies

$$\pi(s) = \prod_{k=0}^m (s - s_k) = s^{m+1} + \mathcal{O}(s^m).$$

Putting these two observations together leads to

$$q(s) = \sum_{l=0}^{\infty} \left(\sum_{k=0}^m w_k s_k^l \right) (s^{m-l} + \mathcal{O}(s^{m-l-1})). \quad (9)$$

The claims of Theorem 3.2 follow from here. Indeed, if (8) is true, then the first ν terms in (9) disappear while the $(\nu + 1)$ -th remains:

$$q(s) = \left(\sum_{k=0}^m w_k s_k^\nu \right) (s^{m-\nu} + \mathcal{O}(s^{m-\nu-1})) + \underbrace{\sum_{l=\nu+1}^{\infty} \left(\sum_{k=0}^m w_k s_k^l \right) (s^{m-l} + \mathcal{O}(s^{m-l-1}))}_{=\mathcal{O}(s^{m-\nu-1})},$$

and $q(s)$ has leading term $(\sum_{k=0}^m w_k s_k^\nu) s^{m-\nu}$, which is nonzero by (8).

On the other hand, if a non-identically-zero q has degree exactly $m - \nu$, then:

- the first ν terms in (9) must disappear, since they have order $> m - \nu$; as such, $\sum_{k=0}^m w_k s_k^l = 0$ for $l = 0, \dots, \nu - 1$;

- the $(\nu + 1)$ -th term in (9) cannot disappear, since all the terms from the $(\nu + 2)$ -th onward have order $< m - \nu$; as such, $\sum_{k=0}^m w_k s_k^\nu \neq 0$.

□

Note that the hypotheses of Theorem 3.2 can be equivalently stated in terms of (generalized) Vandermonde matrices, on which we will rely for building our surrogate model.

Corollary 3.3. *Let $\phi_0(s), \dots, \phi_{\mu-1}(s)$ be any basis of $\mathbb{P}_{\mu-1}(\mathbb{C})$, the space of polynomials of degree $< \mu$. Define $F = \text{diag}(f_0, \dots, f_m) \in \mathbb{C}^{(m+1) \times (m+1)}$ and let*

$$V_{\mu-1} = \begin{bmatrix} \phi_0(s_0) & \cdots & \phi_{\mu-1}(s_0) \\ \vdots & \ddots & \vdots \\ \phi_0(s_m) & \cdots & \phi_{\mu-1}(s_m) \end{bmatrix} \in \mathbb{C}^{(m+1) \times \mu} \quad (10)$$

be the corresponding generalized Vandermonde matrix. If $\mathbf{w} = [w_0, \dots, w_m]^\top$ is nonzero and lies in the null space of $V_{\mu-1}^\top F$, then the exact degree of the numerator of r in (3) is at most $m - \mu$.

Moreover, replacing μ with ν and F with the identity matrix in the previous statement leads to a similar degree condition on the denominator of r : if \mathbf{w} is nonzero and lies in the null space of $V_{\mu-1}^\top$, then the exact degree of the denominator of r in (3) is at most $m - \nu$.

Proof. Define $\mathbf{n} = F\mathbf{w} = [w_0 f_0, \dots, w_m f_m]^\top$, so that, in particular, $V_{\mu-1}^\top \mathbf{n} = V_{\mu-1}^\top F\mathbf{w}$. It is easily seen that the equality conditions in (7) and (8) correspond to null-space constraints for \mathbf{n} and \mathbf{w} , respectively, involving Vandermonde matrices induced by the monomial basis $\phi_l(s) = s^l$, up to degrees $\mu - 1$ and $\nu - 1$, respectively. Since the constraints in (7) and (8) are linear in s_k^l for all k and l , the claim follows by a simple change-of-basis argument (for the polynomial basis). □

4. Rational approximation with given relative degree

The theoretical results from the previous section give us a tool to check the relative degree of a rational function by evaluating linear combinations of its barycentric coefficients. While this can be useful on its own, we can leverage the fact that Theorem 3.2 is a co-implication to design ways of *enforcing* a given degree within rational approximation.

We restrict our attention here to AAA, although the considerations that follow can be generalized to many other rational approximation algorithms, as long as they rely on the barycentric form, cf. Section 6. The plain version of AAA is not concerned with the degree of the rational interpolant r that the algorithm builds. As such, the resulting rational function r will usually have exact type (m, m) . Indeed, round-off errors will generally make both $\sum_{k=0}^m w_k f_k$ and $\sum_{k=0}^m w_k$ nonzero, so that Theorem 3.2 implies the largest possible type, yielding degree 0.

Relying on the results from Section 3, we can prescribe an arbitrary type for the rational approximant by simply adding linear constraints on its barycentric coefficients *during* their computation. For instance, imposing a positive degree $\delta > 0$ leads to

$$\begin{aligned} \min_{w_0, \dots, w_m \in \mathbb{C}} & \sum_{j=1}^{m'} \left| \sum_{k=0}^m \frac{f(s'_j) - f_k}{s'_j - s_k} w_k \right|^2, \\ \text{such that} & \sum_{k=0}^m |w_k|^2 = 1 \\ & \text{and} \quad \sum_{k=0}^m w_k s_k^l = 0 \quad \text{for } l = 0, 1, \dots, \delta - 1. \end{aligned} \quad (11)$$

(Enforcing a degree $\delta < 0$ requires constraints involving $w_k f_k$ instead of just w_k .)

Remark 4.1. It is crucial to observe that the solution of (11) is not *guaranteed* to have exact relative degree δ . Indeed,

- the numerator of r might have degree lower than m (if $\sum_{k=0}^m w_k f_k = 0$);

- the denominator of r might have degree lower than $m - \delta$ (if $\sum_{k=0}^m w_k s_k^\delta = 0$).

(Similar considerations also apply for negative degrees.) However, these are not serious issues, since both above conditions are (i) extremely unlikely due to round-off and (ii) easy to spot. In practice, one might want to return an error message if either $\sum_{k=0}^m w_k f_k$ or $\sum_{k=0}^m w_k s_k^\delta$ is smaller than some tolerance, say 10^{-15} .

Problem (11) can easily be solved by extending ideas from [15, Section 6.2.3]. For instance, following Theorem 3.3, one can recast (11) by restricting (5) to the null space of the (generalized) Vandermonde matrix $V_{|\delta|-1}$, as follows.

First, one computes a matrix $Q \in \mathbb{C}^{(m+1) \times (m+1-|\delta|)}$ with orthonormal columns that span the null space of $V_{|\delta|-1}$. (Note that, if the target degree δ is negative, one must left-multiply the Vandermonde matrix by the diagonal matrix F defined in Theorem 3.3.) To this aim, it suffices, e.g., to extract the rightmost block of the orthogonal matrix resulting from a full QR factorization of $V_{|\delta|-1}$.

Then, one solves the following size- $(m+1-|\delta|)$ problem *without linear constraints*:

$$\min_{v_0, \dots, v_{m-|\delta|} \in \mathbb{C}} \sum_{j=1}^{m'} \left| \sum_{k=0}^m \frac{f(s'_j) - f_k}{s'_j - s_k} \sum_{l=0}^{m-|\delta|} Q_{kl} v_l \right|^2,$$

such that $\sum_{l=0}^{m-|\delta|} |v_l|^2 = 1.$

A solution can be found, e.g., by computing a minimal right singular vector of the matrix LQ , with L being the tall Loewner matrix

$$L = \begin{bmatrix} \frac{f(s'_1) - f_0}{s'_1 - s_0} & \dots & \frac{f(s'_1) - f_m}{s'_1 - s_m} \\ \vdots & \ddots & \vdots \\ \frac{f(s'_{m'}) - f_0}{s'_{m'} - s_0} & \dots & \frac{f(s'_{m'}) - f_m}{s'_{m'} - s_m} \end{bmatrix} \in \mathbb{C}^{m' \times (m+1)}. \quad (12)$$

The desired barycentric coefficients are given by a simple (orthogonal) change of basis: $w_k = \sum_{l=0}^{m-|\delta|} Q_{kl} v_l$.

A pseudo-code summarizing the procedure is provided in Algorithm 1. Differently from the original formulation of AAA [26], we employ the relative error, as opposed to the absolute one, to drive the adaptive selection of the support points and to terminate the sampling loop based on the tolerance ε_{AAA} . Our aim in doing this is to achieve a higher robustness in the approximation of general transfer functions, no matter the underlying system. Indeed, relying on the absolute error behooves one to scale the tolerance on a case-by-case basis, as a way to account for the absolute magnitude of the signal. Another advantage of using the relative error is more specific to our framework: the relative error is more appropriate when the magnitude of the signal displays large variations, e.g., as a result of a nonzero system degree.

Note how, at the m -th iteration, Algorithm 1 imposes an adjusted degree $\text{sign}(\delta) \min\{|\delta|, m\}$, which, for small values of m , may be less (in magnitude) than the target δ . This is out of necessity, since the degree of a rational function cannot be larger than its type.

4.1. Stable extrapolation

By following the strategy described in the previous section, one can build a rational approximation r with an arbitrary relative degree. The surrogate model r can be efficiently and stably evaluated through the barycentric form (2). However, whenever $\text{rdeg}(r) \neq 0$, this stability is guaranteed only at frequencies s located near the sample points. Indeed, if r has a nonzero degree, evaluating it at large frequencies may lead to serious numerical cancellation effects. As detailed in Lemma 4.1 below, the ultimate reason for such cancellation are the identities (7) and (8) in Theorem 3.2, which state that certain linear combinations of the numerator or denominator coefficients equal 0. This is also showcased in Section 7.

Algorithm 1 Data-driven AAA algorithm for rational interpolation (relative error version)

Require: data points $\{(s'_j, f(s'_j))\}_j$, AAA tolerance $\varepsilon_{\text{AAA}} > 0$, target degree $\delta \in \mathbb{N}$

Initialize $\Lambda := \{s'_j\}_j$ and $r := \frac{1}{m'} \sum_{j=1}^{m'} f(s'_j)$
for $m = 0, 1, \dots$ **do**
 Choose $s_m := \arg \max_{s' \in \Lambda} |f(s') - r(s')|/|f(s')|$
 Set $f_m := f(s_m)$ and $\Lambda := \Lambda \setminus \{s_m\}$
if $|f_m - r(s_m)|/|f_m| \leq \varepsilon_{\text{AAA}}$ **then**
 return r
end if
 $\Delta := \min\{|\delta|, m\}$
if $\Delta \neq 0$ **then**
 Assemble the (generalized) Vandermonde matrix $V_{\Delta-1}$ as in (10)
if $\delta < 0$ **then**
 Assemble F as in Theorem 3.3 and update $V_{\Delta-1} := FV_{\Delta-1}$
end if
 Compute a full QR decomposition $\tilde{Q}R := V_{\Delta-1}$
 Define Q as the $(m+1-\Delta)$ rightmost columns of \tilde{Q}
else
 Define Q as the identity matrix of size $(m+1)$
end if
 Assemble the Loewner matrix L in (12) and compute the SVD $U\Sigma V^H := LQ$
 Extract the barycentric coefficients $(w_k)_{k=0}^m$ from the last column of QV
 Define the rational function r as in (2)
end for

This is a serious issue, considering that rational surrogates are often used for forecasting and prediction of systems' frequency responses outside the sampled frequencies. This is even more the case in our paper's setting, since we are focusing on systems whose behavior at $s \rightarrow \infty$ is potentially nonstandard, as encoded by a nonzero relative degree.

To circumvent this problem, we propose a practical strategy relying on *piecewise* approximation, where the surrogate model is evaluated by using one of two formulas: one that is accurate for low frequencies, namely, the barycentric form, (2), and another that is accurate for large frequencies, which we will call "asymptotic form".

The following result provides the foundations for such an asymptotic form for any rational function in barycentric form.

Lemma 4.1. *As in Theorem 3.2, let the non-trivial rational function r in (2) have exact type $(m - \mu, m - \nu)$. As $s \rightarrow \infty$, we have the asymptotic expansion*

$$r(s) = \frac{\sum_{l=0}^{\infty} \left(\sum_{k=0}^m w_k f_k s_k^{\mu+l} \right) s^{-l}}{\sum_{l=0}^{\infty} \left(\sum_{k=0}^m w_k s_k^{\nu+l} \right) s^{-l}} s^{\text{rdeg}(r)}. \quad (13)$$

Proof. By Lemma 3.1, we have the expansions

$$\sum_{k=0}^m \frac{w_k f_k}{s - s_k} = \sum_{l=0}^{\infty} \left(\sum_{k=0}^m w_k f_k s_k^l \right) \frac{1}{s^{l+1}} \quad \text{and} \quad \sum_{k=0}^m \frac{w_k}{s - s_k} = \sum_{l=0}^{\infty} \left(\sum_{k=0}^m w_k s_k^l \right) \frac{1}{s^{l+1}}.$$

By assumption, the first μ (respectively, ν) terms vanish from the sum in the first (respectively, second) identity above. Recalling that $\text{rdeg}(r) = \nu - \mu$, the claim follows by re-indexing the above series and plugging them into the barycentric formula (2). \square

The desired asymptotic form can then be obtained by simply truncating the two series appearing in (13), both having running index l , at some (user-defined) nonnegative order N .

The last ingredient that is needed for our piecewise rational formula is the cutoff radius R_{cutoff} , such that the barycentric, resp. asymptotic, form is used to evaluate $r(s)$ whenever $|s| \leq R_{\text{cutoff}}$,

resp. $|s| > R_{\text{cutoff}}$. While the value of R_{cutoff} may ultimately be selected by a user of our method, we outline here a heuristic way of choosing it in practice.

For this, we compare the extrapolation error incurred with the barycentric form (including effects due to numerical cancellation) with the error that the asymptotic form incurs due to truncation of the series in Lemma 4.1. We choose R_{cutoff} as the frequency s where the two above-mentioned errors are equal. Of course, using the exact errors is unfeasible, as we would need to know the exact, noise-free frequency response at arbitrary frequencies. Instead, we rely on some heuristics.

First, let $T = \max_j |s'_j|$ be the largest frequency for which data is available. When using the barycentric form at large frequencies ($|s| > T$), we assume that the extrapolation error increases following the power law

$$\text{err}_{\text{bary}}(s) \simeq \epsilon \left(\frac{|s|}{T} \right)^{|\text{rdeg}(r)|}. \quad (14)$$

Above, ϵ is an upper bound for the relative approximation error over the frequency region where data is available. For instance, it may be cheaply computed as the largest approximation error over the training dataset. The exponent “ $|\text{rdeg}(r)|$ ” is consistent with Lemma 4.1, as well as with our numerical findings in the next section.

On the other hand, by direct inspection of numerator and denominator of (13), we can verify that the truncation error (at order $l = N$) incurred by the asymptotic form is

$$\text{err}_{\text{asymp}}(s) \simeq \left(\frac{T}{|s|} \right)^{N+1}.$$

For the sake of simplicity, we are assuming the scaling constant in front of the $|s|^{-N-1}$ scaling to be simply T^{N+1} . Again, our numerical tests provide evidence supporting such choice. It is now easy to verify that err_{bary} and $\text{err}_{\text{asymp}}$ are equal at

$$|s| = R_{\text{cutoff}} := T \epsilon^{-1/(|\text{rdeg}(r)|+N+1)}. \quad (15)$$

5. Data-driven identification of the relative degree

In the previous section, we have described how to build a rational approximation with a given degree from available data. However, in the task of *data-driven system identification*, it is often impossible to know the “correct” relative degree in advance: in many settings, the relative degree of the function that generated the frequency-domain data (i.e., the *relative degree* of the underlying dynamical system, cf. Remark 3.1) is unknown. As such, we face the task of identifying such degree from the frequency-domain data.

For this, we rely on *model selection*: first, we approximate the data with several rational functions $\{r^{(\delta)}\}_\delta$ of different relative degrees δ , computed with the strategy outlined in Section 4. Among those, we select the “best” approximation, in a sense to be specified. The relative degree of the selected rational approximation represents our guess for the “exact” relative degree of the underlying system. The only two ingredients that remain to be specified are: (i) how to select the list of potential relative degrees, and (ii) how to choose the “best” rational fit of the data.

A crucial ingredient for answering both questions is a metric to assess the quality of a rational function. Specifically, for our discussion, it is enough to have a criterion to determine which of *two* rational approximations is better. While this will ultimately depend on the specific algorithm used to build the rational functions, cf. Section 6, we describe here a strategy that can be applied in combination with AAA.

Let $r^{(\delta)}$ and $r^{(\delta')}$ be arbitrary rational functions with relative degrees δ and δ' , respectively. We define their corresponding ℓ^∞ approximation errors $e_\infty^{(\delta)}$ and $e_\infty^{(\delta')}$ as the largest (relative) approximation errors achieved by the two functions over the training dataset.

Assuming both $r^{(\delta)}$ and $r^{(\delta')}$ are computed using AAA, it is reasonable to expect their ℓ^∞ approximation errors to be similar. Indeed, both functions’ approximation errors must be below the AAA tolerance ε_{AAA} , which is set in advance. Unable to draw conclusions based on the approximation errors, we assess the quality of a rational approximation based on its “complexity”, i.e., the number $(m+1)$ of terms in its barycentric expansion, cf. (2).

Accordingly, let $(m^{(\bullet)} + 1)$ be the number of barycentric coefficients of $r^{(\bullet)}$. The better rational function is the one with the smaller $m^{(\bullet)}$:

$$r^{(\delta)} \text{ is better than } r^{(\delta')} \text{ iff } \begin{cases} m^{(\delta)} < m^{(\delta')} & \text{if } m^{(\delta)} \neq m^{(\delta')}, \\ |\delta| > |\delta'| & \text{if } m^{(\delta)} = m^{(\delta')} \text{ and } |\delta| \neq |\delta'|, \\ e_{\infty}^{(\delta)} < e_{\infty}^{(\delta')} & \text{if } m^{(\delta)} = m^{(\delta')} \text{ and } |\delta| = |\delta'|. \end{cases} \quad (16)$$

Note that, in case of a tie in complexity but not in degree, we favor the rational function with the larger relative degree (in absolute value) because we consider it the ‘‘simpler’’ model, being more constrained and having fewer free coefficients. Moreover, if both complexity and degree are tied, we fall back to comparing the two rational functions through their approximation error.

We can now describe our model selection algorithm. We begin with a relative degree of $\delta = 0$ and then progressively increment it. As soon as $r^{(\delta)}$ is not better (in the sense of (16)) than $r^{(\delta-1)}$, we stop our search, selecting $r^{(\delta-1)}$ temporarily as the best approximation. This process is then repeated with relative degrees $\delta = -1, -2, \dots$, comparing $r^{(\delta)}$ with $r^{(\delta+1)}$ and stopping as soon as the best approximation $r^{(\delta+1)}$ with non-positive relative degree is found. Finally, the best approximations with positive and negative degrees are compared, and the better one is chosen as the ultimate ‘‘best’’. Some sample pseudo-code for this strategy is provided in Algorithm 2.

Algorithm 2 Data-driven AAA-based degree-identification

Require: data points $D := \{(s'_j, f(s'_j))\}_j$ and AAA tolerance $\varepsilon_{\text{AAA}} > 0$

```

Build baseline  $r^{(0)} := \text{AAA}(D, \varepsilon_{\text{AAA}}, 0)$ 
for  $\delta = 1, 2, \dots$  do
  Build  $r^{(\delta)} := \text{AAA}(D, \varepsilon_{\text{AAA}}, \delta)$  as in Section 4
  if  $r^{(\delta-1)}$  is better than  $r^{(\delta)}$ , cf. (16) then
    Set  $\delta^* := \delta - 1$  and break out of the for-loop
  end if
end for
for  $\delta = -1, -2, \dots$  do
  Build  $r^{(\delta)} := \text{AAA}(D, \varepsilon_{\text{AAA}}, \delta)$  as in Section 4
  if  $r^{(\delta+1)}$  is better than  $r^{(\delta)}$ , cf. (16) then
    Set  $\delta_* := \delta + 1$  and break out of the for-loop
  end if
end for
if  $r^{(\delta^*)}$  is better than  $r^{(\delta_*)}$ , cf. (16) then
  return  $\delta^*$ 
else
  return  $\delta_*$ 
end if

```

6. Extensions to least-squares rational approximation

Although we have focused on AAA throughout the paper, most of our discussion generalizes to any rational approximation strategy that employs the barycentric rational format. Some notable mentions are the vector fitting (VF) algorithm [20], the Antoulas-Anderson (AA) approach [4] and the minimal rational interpolation (MRI) method [29]. As already mentioned in Section 2, VF stands out from the rest because it is not interpolatory, since its support points are chosen not as a subset of the sample points, but through an iterative procedure that aims at progressively improving their location. This lack of interpolation makes VF more robust whenever the data is affected by noise. Indeed, in such cases, the support values f_k used in rational interpolation are affected by noise, generally leading to a lower overall accuracy. For this reason, it is useful to study whether a modification of our data-driven degree-identification approach in Algorithm 2 can be developed, with VF (or other non-interpolatory rational approximation methods) replacing AAA.

First, we note that our theoretical results from Section 3 trivially generalize to rational functions in non-interpolatory barycentric form, as we proceed to state rigorously.

Corollary 6.1. *Theorem 3.2 and Lemma 4.1 remain valid for functions r in barycentric form (1), as long as $w_k f_k$ and w_k are replaced by n_k and d_k , respectively.*

The same is true for Corollary 3.3, although the claim concerning the numerator degree must be stated without involving the matrix F , as “If the vector $\mathbf{n} = [n_0, \dots, n_m]^\top$ is nonzero and lies in the null space of $V_{\mu-1}^\top$, then the exact degree of the numerator of r in (2) is at most $m - \mu$.”

Proof. The claim follows trivially by inspection. \square

Moreover, we recall that, as discussed in Section 2, all the above-mentioned methods rely on a least-squares problem similar to (5), namely, (4), to characterize the approximation’s barycentric coefficients. As such, enforcing a target degree for the rational approximant is just as simple as done in Section 4 for AAA, by restricting the barycentric coefficients to lie in the null space of a suitable (generalized) Vandermonde matrix.

The only part of our discussion that *cannot* be easily generalized to other rational approximation methods is the automatic degree identification presented in Section 5. More specifically, the main difficulty is generalizing criterion (16), which is needed to assess the quality of rational functions and, ultimately, for degree identification. Indeed, (16) uses the complexity of a rational function, as encoded by the number m of its barycentric coefficients, as the main indicator of “badness” of a rational function, neglecting the rational function’s approximation error. This is done by assuming that complexity provides much more information on the quality of a rational function than the approximation error. This is true for AAA, since the method is designed to adaptively explore different complexities. However, most other rational approximation methods (including the above-mentioned ones) *fix* the complexity in advance, thus making it an improper indicator of quality.

One might think that, since complexity is fixed, it might be possible to fall back onto the approximation error as a way to compare rational functions. However, this is not the case, as we proceed to explain. Recall that the barycentric coefficients are found by minimizing the approximation error¹, cf. (5). Any additional degree constraint reduces the size of the “feasible set” where the barycentric coefficients are sought, thus making the minimal value of the target function (i.e., the approximation error) increase. As such, using the approximation error to perform comparisons in Algorithm 2 makes the method always select the default degree-0 rational approximation, it being the one that achieves the smallest error.

As such, it may appear impossible to compare rational functions of different degrees built through, e.g., VF. However, this can be achieved by leveraging a form of model selection. To this aim, we note that VF has already been coupled with model selection strategies [34, 33], as a way to overcome one of its main limitations, namely, the need to fix the “surrogate complexity” m in advance. Without going into too many details, such model selection strategies generally work by using VF to independently build several rational approximations with different values of m , and then selecting the rational approximant characterized by the lowest approximation error². In Section 7.2, we present an alternative way of performing model selection with VF, in a way that mimics AAA more closely.

This means that, given some data, it *is* possible to perform a form of VF where different complexities are adaptively explored, in a flavor similar to AAA, enabling the use of criterion (16) to compare rational functions. Such an “adaptive-complexity” flavor of VF can then be used to replace AAA in our degree-identification strategy, namely, Algorithm 2. Our numerical tests, which can be found in the next section, show that this approach is promising when dealing with noisy data.

¹Admittedly, the rational approximant minimizes the ℓ^2 error through (5), which, in theory, would allow us to use other kinds of error (e.g., the ℓ^∞ one) to compare rational functions without incurring the mentioned error hierarchy. Still, in our experience, imposing degree constraints usually increases *both* ℓ^2 and ℓ^∞ approximation errors, so that the outlined difficulties are still present.

²In this context, one *can* effectively compare rational functions based on their approximation error, since the error is not monotonic with respect to the complexity. This is in contrast with what we mention for our degree-identification routine, where the approximation error behave monotonically with respect to (the absolute value of) the degree.

Test case		Exact relative degree	Sampled frequency range	Relative degree estimate		
				with AAA		with VF
				noiseless	noisy	
Forward 2-mass		-4	$10^{-2} \div 10^0$	✓	✗(0)	✓
Forward 3-mass		-6	$10^{-2} \div 10^0$	✓	✗(-1)	✗(-1)
Inverted 2-mass		4	$10^{-2} \div 10^0$	✓	✓	✓
Inverted 3-mass		6	$10^{-2} \div 10^0$	✗(0)	✗(2)	✗(1)
Oseen flow		1	$10^{-2} \div 10^1$	✓	✗(0)	✓
SLICOT	eady	-1	$10^0 \div 10^3$	✓	✗(-2)	✓
	peec	-1	$10^3 \div 10^4$	✓	✗(0)	✗(-3)
	fom	-1	$10^1 \div 10^2$	✓	✗(0)	✓
	pde	-1	$10^1 \div 10^4$	✓	✗(0)	✓
	heat-disc	-1	$10^0 \div 10^2$	✓	✓	✓
	beam	-1	$10^{-2} \div 10^2$	✓	✓	✓
	mna_1, entry (1, 1)	1	$10^{11} \div 10^{12}$	✓	✓	✓
	mna_1, entry (1, 3)	-1	$10^{11} \div 10^{12}$	✓	✗(0)	✓
	mna_1, entry (2, 3)	1	$10^{11} \div 10^{12}$	✗(-2)	✗(0)	✗(-1)

Table 1: Summary of degree-identification results. Ticks and crosses mark correct and incorrect identifications of the exact relative degrees, respectively. Incorrectly identified degrees are reported in parentheses.

7. Numerical examples

In order to assess the effectiveness of our method, we test it on a plethora of dynamical systems. Specifically, we consider:

- A simple mechanical system that models the elastic interaction of point masses, as illustrated in Figure 5. More details on the model are given in Appendix A. Here it is enough to mention that, given a number $n \geq 2$ of masses, the model comes in two forms: a “forward” model with negative degree $-2n$ and an “inverted” model with positive degree $2n$.
- An Oseen flow problem subject to Dirichlet-type boundary control. The map from the control to the fluid pressure exhibits the characteristics of a DAE of index 2 (degree 1). See, e.g., [18] for the linearized case and [2] for the relevant considerations of the nonlinear Navier-Stokes equations. In our numerical examples, we consider the linear setup described in [18], which models how modulations in the inflow conditions affect pressure measurements in the (linearized) flow past a cylinder at *Reynolds number* $Re = 20$. This example is particularly challenging because its state space is of size $\sim 5 \cdot 10^4$, which makes the acquisition of data rather computationally expensive.
- Many examples from the SLICOT benchmark collection [12], whose relative degrees are either -1 or 1.

As a synthetic way to evaluate our method, we check if it can correctly identify the degree of each of the above-mentioned systems. In all cases, our training samples are located in a very limited frequency band, which is selected case by case, ensuring that the natural frequency of each system is included. In particular, to ensure the fairness of our testing, we tried to select sampling frequencies as low as possible. In this, we are mimicking practical situations where gathering samples at high frequencies is unfeasible, e.g., due to numerical instabilities (for simulated data) or to limitations of the experimental apparatus (for measured data). Obviously, sampling at larger frequencies would have made the task of degree identification simpler, since more information on the frequency-response behavior at $s \rightarrow \infty$ would be available.

The results are shown in Table 1 and are discussed in detail in the upcoming sections. To assess numerical robustness, we use both noiseless and noisy data. The noise is manufactured in a multiplicative way: the j -th data value is perturbed as

$$f_{\text{noisy}}(s'_j) = f(s'_j) \left(1 + 10^{-6} \xi_j\right),$$

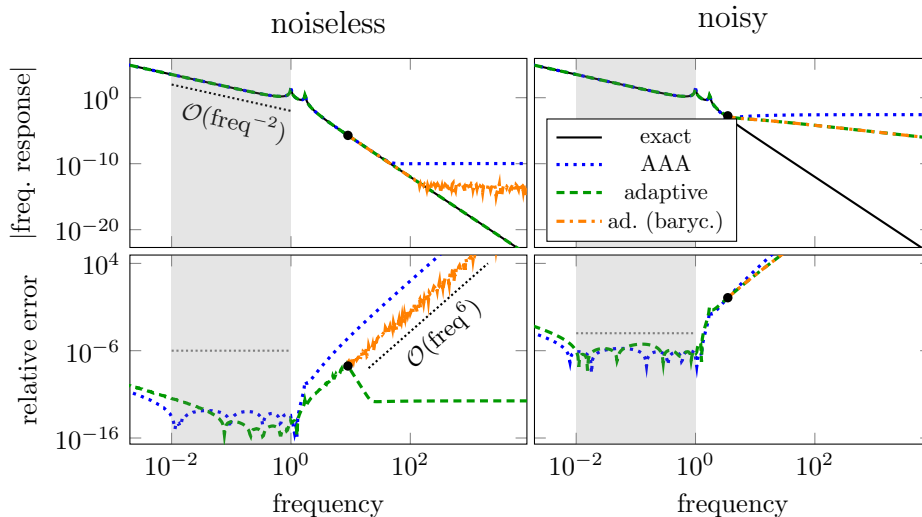


Figure 1: Numerical results for the forward transfer function of the 3-mass chain. The grey band is the sampled frequency range. Black dots denote the point R_{cutoff} , where the barycentric rational form gives way to the asymptotic rational form. The orange dash-dotted curves pertain to the adaptive method’s results using purely the barycentric form.

with ξ_1, ξ_2, \dots being independent samples from a uniform random variable taking values in $[-1, 1]$.

Data Availability The MATLAB code and data files for reproducing the presented experiments are available publicly at [31] under the MIT license and is authored by all three authors.

7.1. Results with AAA

First, we apply our method exactly as presented in Algorithm 2, relying on AAA for rational approximation. We set the AAA tolerance to 10^{-6} and 10^{-4} in the noiseless and noisy cases, respectively. The results are reported in the third-to-last and second-to-last columns of Table 1. We see that our method is generally reliable in the noiseless case, with mostly correct degree identifications across the board. The two failures are discussed and explained in detail below.

When the data is noisy, the algorithm fails in more than two thirds of the tests. This is due to obvious limitations in applying AAA, an interpolatory algorithm, to noisy data. In this sense, we look at the noisy tests’ results as a way to verify that our method *can* work in unfavorable environments, rather than breaking down completely. Indeed, in almost all cases of degree mislabeling due to noise, the degree is underestimated as opposed to overestimated (in magnitude). In fact, our algorithm estimates the degree to be its default zero value in most misidentified cases.

7.1.1. Forward 3-mass system

We now proceed to discuss some selected results in further detail, starting from the noiseless forward 3-mass system. The quality of the approximation can be observed in Figure 1 (left). Our adaptive degree-identification approach is clearly superior to “standard” AAA, with the latter’s approximate frequency response displaying a characteristic saturation at large frequencies, due to its “default” zero relative degree. Note, in particular, how our approach detects the correct relative degree from data on a frequency range where, seemingly, no qualitative indication of the correct degree-(-6) scaling is present: the training data follows much more closely an inverse-quadratic scaling, cf. the reference curve in the top-left plot.

It is interesting to note that, although our approach builds a rational function with the exact relative degree -6 (automatically identified by our algorithm), numerical cancellation in the barycentric form leads to a saturation effect similar to AAA’s. This is evidenced by a drastically increasing approximation error for frequencies larger than 10^1 , in agreement with (14). However,

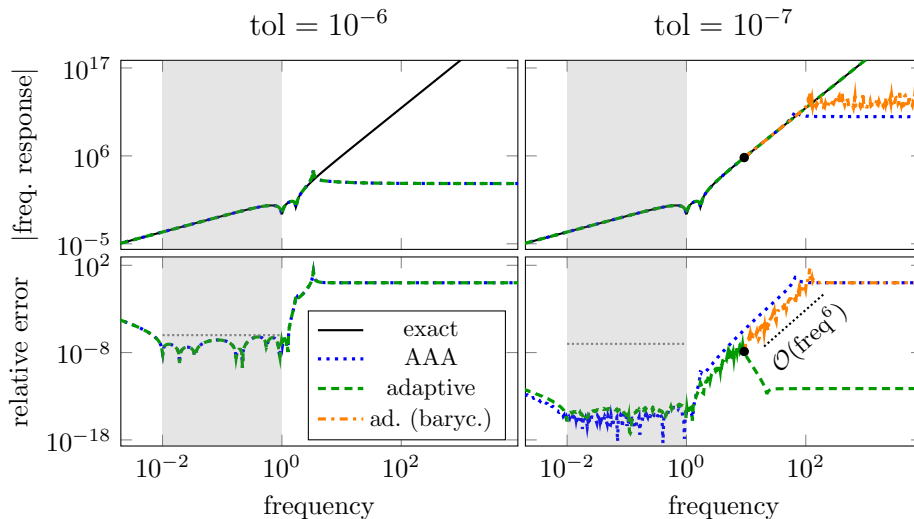


Figure 2: Numerical results for the inverted transfer function of the 3-mass chain. The grey band is the sampled frequency range. Black dots denote the point R_{cutoff} , where the barycentric rational form gives way to the asymptotic rational form. The orange dash-dotted curves pertain to the adaptive method’s results using purely the barycentric form.

the asymptotic form from Lemma 4.1, which we use (with series truncated at $N + 1 = 11$ terms) for frequencies larger than R_{cutoff} (computed as in (15)), manages to recover a stable evaluation even at large frequencies. Still concerning the use of the asymptotic form, we note how the cutoff radius R_{cutoff} is chosen well, ensuring that, at $|s| = R_{\text{cutoff}}$, cancellation errors in the barycentric form are balanced with truncation errors in the asymptotic form.

The results for the noisy case, in Figure 1 (right), are worse, since neither approach is able to correctly identify the correct relative degree of the system. Ultimately, this is due to interpolation of the noise within the sampled frequency range, preventing good extrapolation properties. Specifically for our approach, a correct automatic identification of the degree is hindered by the fact that the noise is spatially uncorrelated, hence difficult to fit with rational functions.

7.1.2. Inverted 3-mass system

We now move to our first failed test, involving the inverted 3-mass system. Since our automatic degree identification returns the default zero degree, the corresponding rational approximation coincides with that obtained by AAA. As shown in Figure 2 (left), the approximation quality quickly degrades as the frequency increases, as a consequence of the badly identified degree.

A closer inspection allowed us to identify why the degree was misidentified. Running “standard” AAA (relative degree $\delta = 0$) with a tolerance of 10^{-6} leads to the selection of 6 support points, with a rational approximant of type (5, 5). However, this is barely enough to attain the tolerance, with the largest approximation error over the sample points being $6.3 \cdot 10^{-7}$. On the other hand, building a rational approximation of type (5, 4) (relative degree $\delta = -1$) attains an error above the tolerance, which makes our algorithm reject positive degrees.

To recover a correct behavior, it was enough to slightly decrease the AAA tolerance to 10^{-7} . We display the corresponding results in Figure 2 (right). This empirically suggests that, with the aim of further increasing the robustness of our approach, it might prove useful to use different AAA tolerances at different stages of the algorithm: a base tolerance for the call to “standard” AAA (relative degree $\delta = 0$) and a slightly larger tolerance for all other calls to AAA with nonzero degree constraints. Note, however, that this modification could make our method more prone to overestimating the degree (in absolute terms).

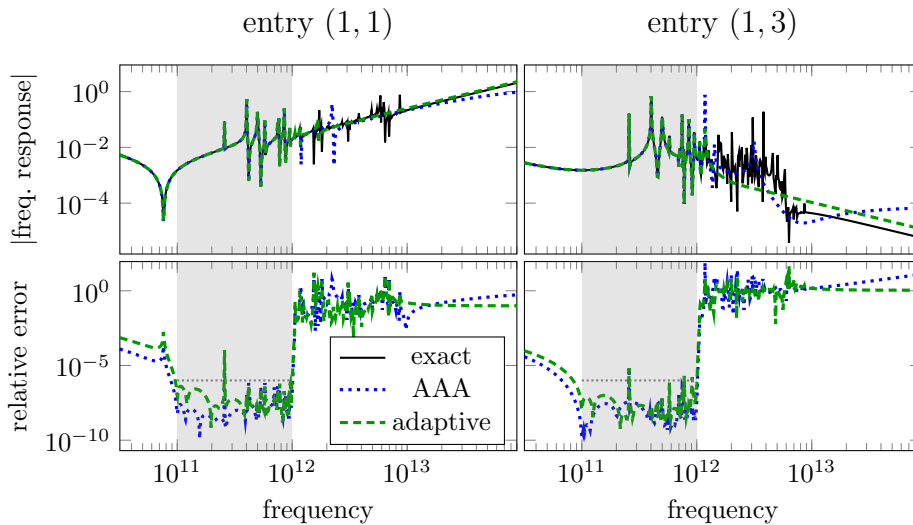


Figure 3: Numerical results for two entries of the MNA_1 transfer-function matrix. The grey band is the sampled frequency range.

7.1.3. SLICOT MNA system

Finally, we look at our other failed test, involving a modified-nodal-analysis system from the SLICOT library [12]. First, as indicated in Table 1, the relative degrees of the (1,1) and (1,3) entries of the transfer-function matrix are correctly identified. This is the case also for most other entries of the transfer function, which we do not include in our showcase for conciseness.

However, as we see in Figure 3, this has no implications on the accuracy of the rational approximation outside the sampled frequency range³. We can observe that large errors are incurred in the secondary peaks of the transfer function. Notably, the asymptotic scaling for large frequencies is well identified, despite errors in the estimation of the *constant in front of the scaling*. These results are quite remarkable since they show how our method is able to decouple *degree identification* from *transfer-function approximation at large frequencies*.

However, there are limitations, as evidenced by the misidentification of the degree of the (2,3) entry of the transfer-function matrix. The corresponding (lack of) approximation accuracy can be observed in Figure 4 (left). This is obviously an example of the above-mentioned decoupling between degree identification and high-frequency transfer-function approximation going wrong. Otherwise stated, the information on a very limited frequency range, which misses some dominant peaks of the transfer function, was not enough to draw correct conclusions on the asymptotic scaling of the transfer function. The simplest way to fix this, recovering a correct degree identification, is to increase the largest sampled frequency. We show in Figure 4 (right) the results for a slightly larger sampling window (the largest sampled frequency is $10^{12.25}$ instead of 10^{12}), which, although not so qualitatively different from the results plotted in Figure 4 (left), display a correct degree identification.

7.2. Results with VF

In Section 6, we discussed how to apply our degree-identification algorithm with least-squares rational approximation, as opposed to interpolation. Non-interpolatory least-squares rational approximation is definitely a more valid choice in the noisy setting. As a way to assess this empirically, we repeat our numerical experiments, replacing AAA with a simplified version of VF.

To build a rational approximation, we fit the data (in a least-squares sense) using VF, although, for the sake of simplicity and to streamline the results, we run a single SK iteration. Given data $\{(s'_j, f(s'_j))\}_{j=1}^{m'}$ from the frequency range $t = |s'_1| \leq \dots \leq |s'_{m'}| = T$, we choose geometrically

³The error is sometimes above the prescribed tolerance even within the sampling range, as a consequence of the fact that we are using a finer frequency grid for making these plots than for training the surrogate.

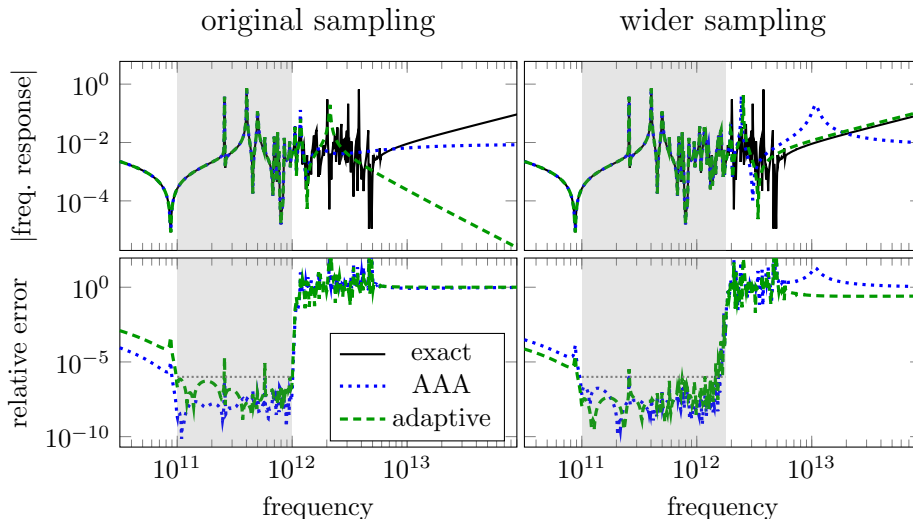


Figure 4: Numerical results for the entry (2,3) of the MNA_1 transfer-function matrix. The grey band is the sampled frequency range.

spaced support points $\{0.9s_1'(1.2T/t)^{k/m}\}_{k=0}^m$. (The scaling factors 0.9 and 1.2 have been added to ensure that the support points are disjoint from the sample points.)

As discussed in Section 6, some form of rational model selection is needed to enable degree identification. In our tests, we perform model selection by progressively increasing the number of support points, until the approximation error is uniformly below a 10^{-4} tolerance. Note how this strategy for model selection, increasing the number of support points until a tolerance is attained, is the same one that is applied in AAA, but without the (in this case) detrimental interpolation property.

The results are reported in the last column of Table 1. We can observe a much higher success rate with respect to AAA, with correct identification of the relative degree in more than two thirds of the test cases. Although we do not present detailed results here, we note that there is numerical evidence to suggest that the degree misidentifications happen mainly because of sampling regions that are too narrow, similarly to what was presented in Section 7.1.3 concerning AAA. Specifically, we have found that enlarging the sampling regions leads to an increased prediction accuracy, as is reasonable to expect.

8. Conclusions

In this paper, we have presented several theoretical results concerning the barycentric rational form, mostly concerning the concept of “relative degree”. Based on such results, we have described two novel numerical algorithms for data-driven system identification.

The first one, Algorithm 1, performs rational approximation while enforcing a prescribed relative degree. Notably, in contrast to other methods, we are able to achieve non-trivial relative degrees without making any modifications to the barycentric rational form, no matter how large the enforced degree.

The second one, Algorithm 2, performs a similar task, but it is the algorithm itself that supplies a guess for the target system’s relative degree. This is achieved through model selection, by leveraging the trade-off between a rational function’s complexity and degree. In contrast to competitor strategies, this degree identification is carried out without the need for high-frequency samples. This latter method has the great advantage of not requiring the user to provide (a guess for) the target system’s relative degree as input. As such, our method can enable degree identifications in settings where no effective alternatives exist, e.g., because an accurate approximation of the transfer function at large frequencies is unfeasible due to the associated sampling/experimental costs.

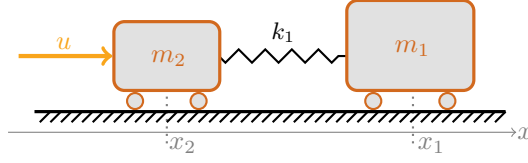


Figure 5: Illustration of the sample mechanical system with $n = 2$ masses.

Our methods' capabilities, in terms of both degree identification and rational approximation, have been showcased through extensive numerical testing. In our tests, we were not able to achieve perfect degree-identification accuracy, especially for noisy data. This is to be expected, since the effectiveness of data-driven methods is ultimately dependent on the quality of the available data. Still, we believe our results to show the great promise of our method. We envision further testing on more challenging engineering applications, so as to better identify strengths and weaknesses of our approach.

At the same time, we believe that it might still be possible to increase the robustness of our method (e.g., to noise in the data) through theoretical means. To this aim, one would have to devise better (heuristic or not) criteria for comparing rational functions of different degrees, compared to those discussed in Sections 5 and 6. At the moment, this remains a future research direction.

A. Mass-train example

Consider two masses that are connected via a spring as illustrated in Figure 5. This mechanical system is modeled with two degrees of freedom, namely, the positions x_1, x_2 . A force of intensity u acts on the second mass and the position x_1 serves as the output y . The model is given as

$$\begin{cases} m_1 \ddot{x}_1 = -k(x_1 - x_2 - d), \\ m_2 \ddot{x}_2 = k(x_1 - x_2 - d) + u, \\ y = x_1. \end{cases}$$

Friction is neglected. On top of the masses m_1 and m_2 , two parameters are present: the spring constant $k > 0$ and the spring length $d > 0$. While the forward problem $u \rightarrow y$ is an integrator chain, the inverted dynamics $y \rightarrow u$ form a DAE of index 5 [1].

In our simulations, we consider the frequency-domain formulation of the generalization of this problem to a chain of $n \geq 2$ masses. We first look at the system

$$\begin{cases} M \ddot{\mathbf{x}} = A \mathbf{x} + \mathbf{f} + B u, \\ y = C \mathbf{x}. \end{cases}$$

Above, $\mathbf{x} = [x_1, \dots, x_n]^\top$ is the vector of the masses' coordinates, the mass values are merged into $M = \text{diag}(m_1, \dots, m_n) \in \mathbb{R}^{n \times n}$, while

$$A = \begin{bmatrix} -k_1 & k_1 & & & & & \\ k_1 & -k_1 - k_2 & k_2 & & & & \\ & \ddots & \ddots & \ddots & & & \\ & & & k_{n-2} & -k_{n-2} - k_{n-1} & k_{n-1} & \\ & & & & k_{n-1} & -k_{n-1} & \end{bmatrix}, \quad \mathbf{f} = \begin{bmatrix} k_1 d_1 \\ -k_1 d_1 + k_2 d_2 \\ \vdots \\ -k_{n-2} d_{n-2} + k_{n-1} d_{n-1} \\ -k_{n-1} d_{n-1} \end{bmatrix},$$

$B = [0, 0, \dots, 0, 1]^\top \in \mathbb{R}^{n \times 1}$, and $C = [1, 0, \dots, 0, 0] \in \mathbb{R}^{1 \times n}$. The spring constants $k_1, \dots, k_{n-1} > 0$ and spring lengths $d_1, \dots, d_{n-1} > 0$ are arbitrary, although, in our numerical tests, we set all constants to 1: $m_j = k_j = d_j = 1$ for all j .

In the frequency domain, the $u \rightarrow y$ map is obtained as an affine linear (with respect to u) map

$$y(s) = C(s^2 M - A)^{-1} \left(B u(s) + \frac{1}{s} \mathbf{f} \right) \quad (17)$$

and the inverted map $y \rightarrow u$ as

$$u(s) = (C(s^2M - A)^{-1}B)^{-1} \left(y(s) - C(s^2M - A)^{-1} \frac{1}{s} \mathbf{f} \right). \quad (18)$$

As the affine part can be estimated separately, in the numerical tests, we will only consider the linear part of the transfer function. Otherwise stated, we set $d_1 = \dots = d_{n-1} = 0$, so that $\mathbf{f} = \mathbf{0}$ in (17) and (18).

References

- [1] R. Altmann and J. Heiland. Simulation of multibody systems with servo constraints through optimal control. *Multibody System Dynamics*, 40(1):75–98, 2017. doi:10.1007/s11044-016-9558-z.
- [2] R. Altmann and J. Heiland. Continuous, semi-discrete, and fully discretized Navier-Stokes equations. In Stephen Campbell, Achim Ilchmann, Volker Mehrmann, and Timo Reis, editors, *Applications of Differential-Algebraic Equations: Examples and Benchmarks*, Differential-Algebraic Equations Forum, pages 277–312. Springer, 2019. doi:10.1007/11221_2018_2.
- [3] A. C. Antoulas. *Approximation of Large-Scale Dynamical Systems*, volume 6 of *Adv. Des. Control*. SIAM Publications, Philadelphia, PA, 2005. doi:10.1137/1.9780898718713.
- [4] A. C. Antoulas and B. D. O. Anderson. On the scalar rational interpolation problem. *IMA J. Math. Control. Inf.*, 3(2-3):61–88, 1986. doi:10.1093/imamci/3.2-3.61.
- [5] A. C. Antoulas, I. V. Gosea, and M. Heinkenschloss. Data-driven model reduction of the Oseen equations using the Loewner framework. In S. Grundel, T. Reis, and S. Schöps, editors, *Progress in Differential-Algebraic Equations II*, Differential-Algebraic Equations Forum, pages 185–210. Springer, 2020. doi:10.1007/978-3-030-53905-4_7.
- [6] Q. Aumann, P. Benner, I. V. Gosea, J. Saak, and J. Vettermann. A tangential interpolation framework for the AAA algorithm. *Proc. Appl. Math. Mech.*, 23(3):e202300183, 2023. doi:10.1002/pamm.20230183.
- [7] P. J. Baddoo. The AAAtrig algorithm for rational approximation of periodic functions. *SIAM J. Sci. Comput.*, 43(5):A3372–A3392, 2021. doi:10.1137/20M1359316.
- [8] P. Benner and T. Stykel. Model order reduction for differential-algebraic equations: A survey. In Achim Ilchmann and Timo Reis, editors, *Surveys in Differential-Algebraic Equations IV*, Differential-Algebraic Equations Forum, pages 107–160. Springer International Publishing, Cham, March 2017. doi:10.1007/978-3-319-46618-7_3.
- [9] T. Berger, A. Ilchmann, and E. P. Ryan. Funnel control – a survey, 2023. arXiv:2310.03449.
- [10] J.-P. Berrut and H. D. Mittelmann. Matrices for the direct determination of the barycentric weights of rational interpolation. *J. Comput. Appl. Math.*, 78(2):355–370, 1997. doi:10.1016/S0377-0427(96)00163-X.
- [11] J.-P. Berrut and L. N. Trefethen. Barycentric Lagrange interpolation. *SIAM Rev.*, 46(3):501–517, 2004. doi:10.1137/S0036144502417715.
- [12] Y. Chahlaoui and P. Van Dooren. A collection of benchmark examples for model reduction of linear time invariant dynamical systems. Technical Report 2002–2, SLICOT Working Note, 2002. Available from www.slicot.org.
- [13] L. Davis, W. Johns, L. Monzon, and M. Reynolds. Iterative stability enforcement in Adaptive Antoulas-Anderson algorithms for H_2 model reduction. *SIAM J. Sci. Comput.*, 45(4), 7 2023. doi:10.1137/21M1467043.
- [14] S. Elsworth and S. Güttel. Conversions between barycentric, RKFUN, and Newton representations of rational interpolants. *Lin. Alg. Appl.*, 576:246–257, 2019. doi:10.1016/j.laa.2018.10.003.
- [15] G. H. Golub and C. F. Van Loan. *Matrix Computations*. Johns Hopkins University Press, Philadelphia, PA, 4th edition, 2013. doi:10.1137/1.9781421407944.
- [16] I. V. Gosea and S. Gugercin. Data-driven modeling of linear dynamical systems with quadratic output in the AAA framework. *J. Sci. Comput.*, 91(1):1–28, 2022. doi:10.1007/s10915-022-01771-5.
- [17] I. V. Gosea and S. Güttel. Algorithms for the rational approximation of matrix-valued functions. *SIAM J. Sci. Comput.*, 43(5):A3033–A3054, 2021. doi:10.1137/20m1324727.

-
- [18] I. V. Gosea and J. Heiland. Implicit and explicit matching of non-proper transfer functions in the Loewner framework. In *2024 European Control Conference (ECC)*, pages 3452–3457, 2024. doi:[10.23919/ECC64448.2024.10590815](https://doi.org/10.23919/ECC64448.2024.10590815).
- [19] I. V. Gosea, Q. Zhang, and A. C. Antoulas. Preserving the DAE structure in the Loewner model reduction and identification framework. *Adv. Comp. Math.*, 46(3), 2020. doi:[10.1007/s10444-020-09752-8](https://doi.org/10.1007/s10444-020-09752-8).
- [20] B. Gustavsen and A. Semlyen. Rational approximation of frequency domain responses by vector fitting. *IEEE Trans. Power Del.*, 14(3):1052–1061, 1999. doi:[10.1109/61.772353](https://doi.org/10.1109/61.772353).
- [21] S. Güttel, D. Kressner, and B. Vandereycken. Randomized sketching of nonlinear eigenvalue problems. *SIAM J. Sci. Comput.*, 46(5):A3022–A3043, 2024. doi:[10.1137/22M153656X](https://doi.org/10.1137/22M153656X).
- [22] S. Güttel, G. M. Negri Porzio, and F. Tisseur. Robust rational approximations of nonlinear eigenvalue problems. *SIAM J. Sci. Comput.*, 44(4):A2439–A2463, 2022. doi:[10.1137/20M1380533](https://doi.org/10.1137/20M1380533).
- [23] A. Isidori. *Nonlinear Control Systems*, volume 72 of *Lect. Notes Control Inf. Sci.* Springer, 3 edition, 1985. doi:[10.1007/978-1-84628-615-5](https://doi.org/10.1007/978-1-84628-615-5).
- [24] P. Kunkel and V. Mehrmann. *Differential-algebraic equations: analysis and numerical solution*, volume 2. European Mathematical Society, 2006. doi:[10.4171/017](https://doi.org/10.4171/017).
- [25] P. Lietaert, K. Meerbergen, J. Pérez, and B. Vandereycken. Automatic rational approximation and linearization of nonlinear eigenvalue problems. *IMA J. Numer. Anal.*, 42(2):1087–1115, 2022. doi:[10.1093/imanum/draa098](https://doi.org/10.1093/imanum/draa098).
- [26] Y. Nakatsukasa, O. Sete, and L. N. Trefethen. The AAA algorithm for rational approximation. *SIAM J. Sci. Comput.*, 40(3):A1494–A1522, 2018. doi:[10.1137/16M1106122](https://doi.org/10.1137/16M1106122).
- [27] F. Nobile and D. Pradovera. Non-intrusive double-greedy parametric model reduction by interpolation of frequency-domain rational surrogates. *ESAIM: Mathematical Modelling and Numerical Analysis*, 55(5), 2021. doi:[10.1051/m2an/2021040](https://doi.org/10.1051/m2an/2021040).
- [28] L. Petzold. Differential/algebraic equations are not ODE’s. *SIAM J. Sci. Stat. Comput.*, 3(3):367–384, 1982. doi:[10.1137/0903023](https://doi.org/10.1137/0903023).
- [29] D. Pradovera. Interpolatory rational model order reduction of parametric problems lacking uniform inf-sup stability. *SIAM J. Numer. Anal.*, 58(4):2265–2293, 2020. doi:[10.1137/19M1269695](https://doi.org/10.1137/19M1269695).
- [30] D. Pradovera. Adaptive approximation of nonlinear eigenproblems by minimal rational interpolation. *Proc. Appl. Math. Mech.*, 22(1), 2023. doi:[10.1002/pamm.202200032](https://doi.org/10.1002/pamm.202200032).
- [31] D. Pradovera, I. V. Gosea, and J. Heiland. Code, data, and results for numerical experiments in “Barycentric rational approximation for learning the index of a dynamical system from limited data” (version 1.0), September 2024. doi:[10.5281/zenodo.1383801](https://doi.org/10.5281/zenodo.1383801).
- [32] A. Carracedo Rodriguez, L. Balicki, and S. Gugercin. The p-AAA algorithm for data driven modeling of parametric dynamical systems. *SIAM J. Sci. Comput.*, 45(3):A1332–A1358, 2023. doi:[10.1137/20M1322698](https://doi.org/10.1137/20M1322698).
- [33] T. Vojkovic, D. Quero, C. Poussot-Vassal, and P. Vuillemin. Low-order parametric state-space modeling of MIMO systems in the Loewner framework. *SIAM J. Appl. Dyn. Syst.*, 22(4):3130–3164, 2023. doi:[10.1137/22M1509898](https://doi.org/10.1137/22M1509898).
- [34] Y. Q. Xiao, S. Grivet-Talocia, P. Manfredi, and R. Khazaka. A novel framework for parametric loewner matrix interpolation. *IEEE Trans. Compon. Packag. Manuf. Technol.*, 9(12):2404–2417, 2019. doi:[10.1109/TCPMT.2019.2948802](https://doi.org/10.1109/TCPMT.2019.2948802).